Model Predictive Control for Starvation Prevention in a Hybrid Fuel Cell System[1]

Ardalan Vahidi [2] Anna Stefanopoulou Huei Peng
Mechanical Engineering, University of Michigan, Ann Arbor

Abstract

When current is drawn from a fuel cell, it is critical that the reacted oxygen is replenished rapidly by the air supply system to avoid stack starvation and damage. We first explain that in a stand-alone fuel cell, there is lack of control authority in avoiding excessive oxygen starvation during high current demand. In the hybrid configuration introduced in this paper, a small auxiliary power source significantly extends the control authority in avoiding oxygen starvation. To achieve best possible results without violating operational constraints of the system, a well-devised current split strategy is required. We formulate distribution of current demand between the fuel cell and the auxiliary source in a constrained optimization (model predictive control) framework. As a result, the reactant deficit during sudden increases in stack power was reduced from 50% in stand-alone architecture to less than 1% in the hybrid configuration.

1 Introduction

Increased environmental awareness, advances in power electronics, more efficient electric motors, and breakthroughs in membrane and electrode technologies have raised the interest and investment in fuel cell research. A fuel cell power system requires the integration of many components beyond the fuel cell stack itself, to allow efficient performance under different operating conditions. A system must be built around the fuel cell stack to supply air and fuel, remove the depleted reactants and heat that are produced by the reactions in the cells and convert the generated DC power to regulated DC or grid quality AC power. To maintain efficiency and avoid degradation of available fuel cell voltage, a control system is necessary for maintaining optimal temperature, membrane humidity and pressure of reactants across the membrane. The design and optimization of the fuel cell auxiliary system is complex because of the interaction between all the performance variables and varying operating conditions.

The supply of oxygen to the cathode is one of the key factors in operation of a fuel cell stack and is the subject of this paper. When current is drawn from a fuel cell, the air supply system should replace the reacted oxygen. Otherwise the cathode will suffer from oxygen starvation which damages the stack and limits the power response of the fuel cell. In high-pressure fuel cells a compressor motor is used to provide the required air into the cathode through a manifold. The challenge is that oxygen reacts instantaneously as current is drawn from the stack, while the air supply rate is limited by the manifold dynamics and compressor operational constraints. Figure 1 shows a schematic of a fuel cell stack and air supply system. In [1], Pukrushpan et al. have shown that a combination of feedback and feedforward control of the compressor input, can improve the transient oxygen response. However

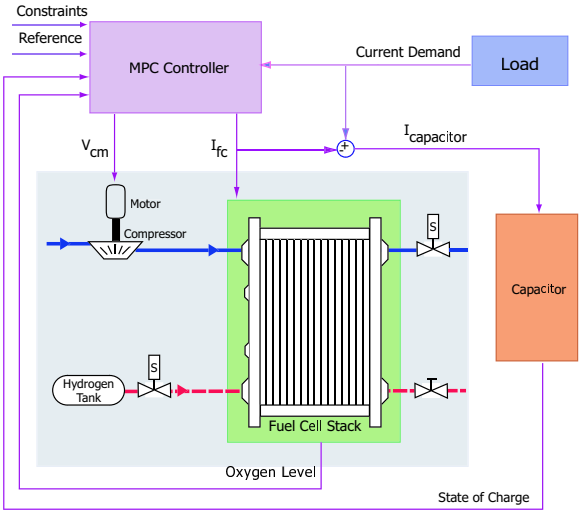

Figure 1: Schematic of the fuel cell stack and air supply control system. The fuel cell stack consists of 350 cells with peak power of 75kw. The high pressure air supply is powered by a 12kw compressor.

the drop in oxygen level could not be completely eliminated by merely relying on the compressor unless the intention to change the load levels is known in advance. Figure 2 shows this limitation, during a step change of 100 Amps in current demand. It is shown that the oxygen excess ratio drops initially from its desired value of 2 to almost 1.0.

To remedy this limitation, Sun and Kolmanovsky [2] propose using a "load governor" for starvation prevention. The load governor controls the current drawn from the fuel cell to ensure that constraints on oxygen level are fulfilled. Basically, the governor acts as a dynamic filter preceeding the closed loop system which delays the current command slightly but preserves the tracking capability and disturbance rejection of the linear system [3].

To avoid starvation and simultaneously match an arbitrary level of current demand, adding a rechargeable auxiliary power source which can respond quickly to the increase in current demand is necessary. A battery or an ultra-capacitor for example, are power sources that respond relatively quickly to current demand. They can be used in parallel with a fuel cell to cover the high peaks in demand and can be recharged by the fuel cell itself, when the demand is lower. In this paper, we use model predictive control for air flow management in a hybrid fuelcell-ultracapacitor system. MPC finds an optimum balance between use of fuel cell and capacitor during fast current transients and facilitates enforcement of bounds on capacitor's state of charge. Moreover, in contrast to methodologies like dynamic programming, MPC does not require the knowledge of the load cycle. The predictive nature of MPC and its receding horizon, result in smooth transitions between use of

[1]This work is funded by NSF 0201332 and the Automotive Research Center (ARC) under U.S. Army contract DAAE07-98-3-0022.

[2]Corresponding Author, G008 Walter E. Lay Auto Lab, The University of Michigan, 1231 Beal Avenue, Ann Arbor, MI, 48109, avahidi@umich.edu

the capacitor and the fuel cell, despite the unknown load cycle. The smooth performance and capability to handle constraints have been our key motivation for using model predictive control to optimally split the current demand between the fuel cell and the auxiliary power source.

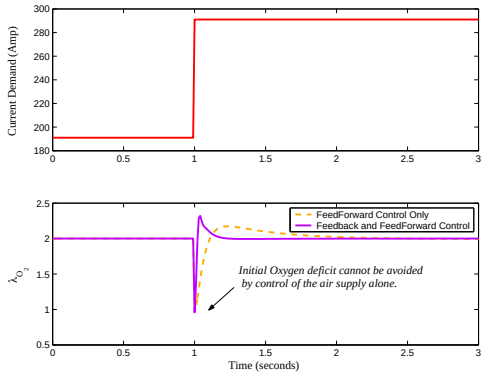

Figure 2: Change of oxygen level in the cathode in a stand-alone fuel cell during a step change of 100 Amps in demand.

A literature search shows that load management between two power sources (typically internal combustion engine and battery) is formulated as power split instead of current split. Specifically, power split methods in hybrid electric systems literature have two categories: (i) "Rule-based" in which power splitting is based on instant demand [4, 5]. The advantage of these methods is their relative simplicity. However they do not guarantee optimal use of the resources over a working cycle. (ii) "Optimization-based" methods on the other hand, optimize over a longer decision horizon and therefore are less likely to suffer from "short-sighted" decisions. Dynamic programming (DP) is one of the optimization-based approaches that has been used for power management of hybrid electric vehicles. In most scenarios dynamic programming is used offline for a given load cycle and therefore is cycle specific [6, 7]. However rules can be devised based on the insight obtained from a DP approach [6]. Hybrids of fuel-cell with batteries or ultra-capacitors have also been considered for increased efficiency in automotive [8, 9] or other applications [10]. Paganelli et al. have used an optimal control design to minimize the use of hydrogen in a hybrid fuel cell system [11]. Their design ensures that the auxiliary power source is charged at the end of each cycle. If upper and lower bounds can be enforced on the state of charge of the auxiliary power source throughout the cycle, then the size of the auxiliary power source can be reduced, with direct benefits to vehicle performance. Bounds on state of charge can be best described with active inequality constraints. Finding closed-form solution to the optimal control problem with such inequality constraints is not feasible in general. Model Predictive Control is an optimal control methodology which incorporates such constraints in control design and optimization by online optimization of a quadratic program.

In this paper, we first explain the dynamic model of the fuel cell system, followed by a description of the hybrid fuelcell-ultracapacitor architecture. We then formulate the MPC design and select the suitable control parameters in linear analysis. Finally we demonstrate simulation results for both linear and nonlinear systems in constrained conditions.

2 Model of the Fuel Cell System

A nonlinear model of a fuel cell stack together with its auxiliaries is developed in [12] based on electrochemical, thermodynamic and fluid flow principles. The model is detailed on aspects which are most critical for control design in automotive applications. Models are developed for the compressor, manifold dynamics, cooling system, the humidifier, membrane hydration, anode and cathode flow and stack voltage. Augmenting these subsystems formed a nonlinear model of the fuel cell system. Since the focus in this paper is control of air flow, we present the governing equations, essential to understanding the dynamics between the compressor and the air flow into the cathode. The interested reader can find more details about the model in [1, 12].

Low partial oxygen pressure in the cathode decreases the fuel cell voltage and the generated power and can reduce the life of the stack. To prevent such a situation the oxygen level in the cathode needs to be regulated. By neglecting the spatial variations and assuming homogeneous oxygen concentration throughout the cathode, a single parameter can be defined to indicate the oxygen level status in the cathode. Oxygen excess ratio (OER), λ_{O_2}, is defined for this purpose as follows:

$$\lambda_{O_2} = \frac{W_{O_2,in}}{W_{O_2,rct}} \tag{1}$$

where $W_{O_2,in}$ is the of flow of oxygen into the cathode and $W_{O_2,rct}$ is the mass of oxygen reacted in the cathode. Therefore low values of λ_{O_2} is an indication of oxygen starvation. The rate of oxygen reacted, $W_{O_2,rct}$, depends on the current drawn from the stack, I_{fc}:

$$W_{O_2,rct} = M_{O_2}\frac{nI_{fc}}{4F} \tag{2}$$

where n is the number of cells in the stack and F is the Faraday number (F=96485 Coulombs). Therefore with increase in current drawn from the fuel cell, λ_{O_2} decreases. To maintain the level of OER, more air should be supplied to the fuel cell. The flow rate of the oxygen into the stack, $W_{O_2,in}$, is a function of the air flow out of the supply manifold, W_{sm}:

$$W_{O_2,in} = y_{O_2}\frac{1}{1+\Omega_{atm}}W_{sm} \tag{3}$$

where $y_{O_2} = 0.21\frac{M_{O_2}}{M_a^{atm}}$ is the mass ratio of oxygen in the dry atmospheric air and Ω_{atm} is the humidity ratio of the atmospheric air. The mass flow rate out of the supply manifold, W_{sm}, depends on the downstream (cathode) pressure and upstream (supply manifold) pressure, p_{sm}, and temperature, T_{sm}. The cathode total pressure depends on the partial pressure of the (i) oxygen that is supplied, $W_{O_2,in}$, reacted, $W_{O_2,rct}$, and the oxygen removed, (ii) nitrogen that is supplied and removed and (iii) the water that is supplied, generated, transported through the membrane and removed. The additional cathode states of oxygen mass, m_{O_2}, nitrogen mass, m_{N_2}, water vapor mass, $m_{w,ca}$, total return manifold pressure, p_{rm}, and anode states of hydrogen mass, m_{H_2}, and water vapor, $m_{w,an}$, are needed to capture the temporal dynamics of the total cathode pressure during a step change in current, I_{fc}. These detailed state equations are omitted here but can be found in [12]. However, to allow the reader understand how the control input affects the supply manifold flow, W_{sm}, we add the following relations. Specifically the supply manifold pressure, p_{sm}, and mass, m_{sm}, are related to the compressor's air flow, W_{cp}, and temperature, T_{cp}, with the following dynamics:

$$\frac{dp_{sm}}{dt} = K_{sm}(W_{cp}T_{cp} - W_{sm}T_{sm}) \tag{4}$$

$$\frac{dm_{sm}}{dt} = W_{cp} - W_{sm} \tag{5}$$

where K_{sm} is a coefficient determined by air specific heat coefficients and the manifold volume. The supply manifold temperature, T_{sm}, is

defined by the ideal gas law. The compressor air flow, W_{cp}, and its temperature, T_{cp}, depend on the compressor rotational speed, ω_{cp}:

$$J_{cp}\frac{d\omega_{cp}}{dt} = \frac{1}{\omega_{cp}}(P_{cm} - P_{cp}) \tag{6}$$

where J_{cp} is the compressor inertia and P_{cp} is the power absorbed by the compressor. The power supplied to the compressor, P_{cm}, is a function of compressor motor voltage, V_{cm}.

In summary, the compressor voltage, V_{cm}, controls the speed of the compressor through the first-order nonlinear dynamics shown in (6). Speed of the compressor determines the compressor flow rate, W_{cp}, which then through equation (4) affects the supply manifold pressure, p_{sm}, which together with the cathode pressure, determines the supply manifold flow, W_{sm}, and finally flow rate of the oxygen into the cathode, $W_{O_2,in}$.

The set of equations described above, form a set of first-order nonlinear differential equations:

$$\begin{aligned} \dot{x}_{nl} &= h(x_{nl}, u, w) \\ u &= [V_{cm} \quad I_{fc}]^T \\ y &= \lambda_{O_2} \end{aligned} \tag{7}$$

where x_{nl} is the state vector of the nonlinear dynamic system from $u = [V_{cm} \quad I_{fc}]^T$ to $y = \lambda_{O_2}$, oxygen excess ratio, which we assume is measured.[1] For the control design purpose, this augmented nonlinear system is linearized around a selected operating point. We define nominal stack current of I^0_{fc}. The nominal value for oxygen excess ratio is selected at $\lambda^0_{O_2} = 2.0$, which corresponds to maximum fuel cell net power for the nominal current [12]. The compressor motor voltage needed, to supply the optimum air flow that corresponds to I^0_{fc} and $\lambda^0_{O_2} = 2.0$, is $V^0_{cm} = 164$ volts. The linearized system has eight dynamic states and is described by:

$$\begin{aligned} \dot{x}_{ln} &= Ax_{ln} + Bu \\ y &= Cx_{ln} + Du \end{aligned} \tag{8}$$

where the variables x_{ln} and y show deviations from their nominal values. The linear state vector is:

$$x_{ln} = [m_{O_2} \quad m_{H_2} \quad m_{N_2} \quad w_{cm} \quad p_{sm} \quad m_{sm} \quad m_{w,an} \quad p_{rm}]^T_\delta$$

A discretized version of this linear model is used for control design in this paper. The nonlinear model (7) is used in nonlinear closed-loop simulations. Addition of an ultra-capacitor is explained in the next section.

3 The Hybrid FuelCell-UltraCapacitor Configuration

In absence of an auxiliary power source, the current drawn from the fuel cell acts as an external disturbance and its sudden increase results in oxygen starvation. By adding a fast power source, part of the power demand during peaks can be drawn from the auxiliary source, giving the fuel cell and the compressor time to adjust to the new power levels. To respond to rapid increase in demand, the auxiliary power source should be able to deliver high powers for short periods of time. Batteries can not provide such instantaneous power. The requirement is best achieved by an ultra-capacitor. Ultracapacitors have an energy density up to a hundred times higher than conventional capacitors. Their power density is up to ten times higher than batteries [8]. The capacitor is recharged by the fuel cell when the demand is not violating the oxygen constraints. As a result critical starvation conditions can be avoided during sudden increase in demand. A controller adjusts the compressor input and current split proportion to regulate oxygen level and state of charge of the auxiliary power source. The assumption is that the response time of the auxiliary power source is considerably faster than the response time of the fuel cell. If the current demand is feasible, that is if it does not exceed the capacity of the hybrid system, it can always be met by the fuel cell or combination of fuel cell and the ultra-capacitor as follows:

$$I_{des} = I_{fc} + I_{capacitor} \tag{9}$$

where I_{des} is the total requested current, I_{fc} is the part provided from the fuel cell, and $I_{capacitor} = I_{des} - I_{fc}$, is provided by the capacitor when positive. Negative $I_{capacitor}$ means that the fuel cell is charging the capacitor. The charging current would then be a positive $I_{fc} - I_{des}$.

The change in charge of a capacitor is proportional to the charging current. The "state of charge" of the capacitor is defined as [13]:

$$SOC(k+1) = SOC(k) + \beta(I_{fc} - I_{des})$$

and is a normalized measure based on its maximum charge. Specifically $SOC = 1$ corresponds to capacitors maximum charge and $SOC = 0$ corresponds to the minimum charge. The parameter β, is a constant and depends on the size and number of capacitors used. In this work, we chose $\beta = 2.77 \times 10^{-4} \frac{1}{Amp}$, which corresponds to a small power buffer required for starvation prevention. One possible configurations that realizes this value of β, is a bank of 100 capacitors, each with capacitance of 10 Farads and a rated voltage of 3 volts, connected in series. Performance characteristics of typical capacitors of this size are shown in table 4 of [14]. Together the package of capacitors can provide a voltage of 300 volts and a storage capacity of 1.25 watt-hours. Total net weight of the bank of capacitors is in the range of one kilogram according to the specifications provided in [14]. The capacitors are used for a fraction of a second to shield the fuel cell from starvation.[2]

For the optimization process it is more convenient if we define "state of discharge" instead of state of charge:

$$SD(k) = 1 - SOC(k)$$

Minimization of state of discharge translates to recharge of the capacitor. Therefore:

$$SD(k+1) = SD(k) - \beta(I_{fc} - I_{des}) \tag{10}$$

This equation is coupled with the fuel cell state equations (8), through the I_{fc} term and results in the following augmented system:

$$x_a(k+1) = \begin{bmatrix} A & 0 \\ 0 & 1 \end{bmatrix} x_a(k) + \begin{bmatrix} D \\ -\beta \end{bmatrix} u(k) + \begin{bmatrix} 0 \\ \beta \end{bmatrix} w(k) \tag{11}$$

The augmented state vector, x_a, control input, u, and disturbance w(k) are:

$$x_a(k) = \begin{bmatrix} x_{ln}(k) \\ SD(k) \end{bmatrix} \quad u(k) = \begin{bmatrix} V_{cm}(k) \\ I_{fc}(k) \end{bmatrix} \quad w(k) = I_{des}$$

[1] Oxygen excess ratio cannot be directly measured in practice. An observer could be used to reconstruct it from other measurements. Potential possible measurements are air flow rate through the compressor, W_{cp}, supply manifold pressure, p_{sm}, and stack voltage, V_{st} as shown in [1, 12].

[2] Rodatz et al. have used ultra capacitors in a hybrid fuel cell vehicle for peak power levelling to assist the fuel cell during hard accelerations and for storing the energy from regenerative braking [8]. A much larger buffer size is required for their purpose. They have provided this buffer by 282 pair-wise connected capacitors, each with capacitance of 1600F.

The outputs of interest are oxygen excess ratio and state of discharge. The output vector $y_a(k) = [\lambda_{O_2}(k) \quad SD(k)]^T$ can be written as follows:

$$y_a(k) = \begin{bmatrix} C & 0 \\ 0 & 1 \end{bmatrix} x_a(k) + \begin{bmatrix} D \\ 0 \quad 0 \end{bmatrix} u(k) \tag{12}$$

In this hybrid architecutre, the disturbance is the total current demand, I_{des}, and is treated as a measured disturbance. We require that the oxygen excess ratio and state of charge of the capacitor always remain within specified limits. To address this control problem, we use a model predictive control (MPC) scheme to regulate the oxygen level and capacitor's state of charge. Formulation of the MPC methodology used in this work is similar to what is detailed in [15]. For completeness, the essential MPC equations in their general form are highlighted next.

4 Formulation of the MPC scheme

MPC is based on minimization of a performance index of the predicted response of a system over a future horizon. A brief summary is provided next. Our notations follow [16]. For more details see [15]. We assume the plant equations are in general nonlinear with the nonlinear state-space representation:

$$\begin{aligned} x_p(k+1) &= f_{nl}(x_p(k), u(k), w_m(k), w_u(k)) \\ y_p(k) &= g_{nl}(x_p(k), w_m(k)) + w_y(k) \end{aligned} \tag{13}$$

where x_p and y_p are states and output of the plant, u is the control input, w_m and w_u represent measured and unmeasured disturbances respectively and $w_y(k)$ is output disturbance. The model used for prediction and control design is called the internal model which is usually a simplified version of the plant model. In a linear MPC design, which we study in this paper, the internal model is a linearized model of the plant in the following form:

$$\begin{aligned} x(k+1) &= Ax(k) + B_u u(k) + B_{wm} w_m(k) + B_{wu} w_u(k) \\ y(k) &= Cx(k) + D_{wu} w_u(k) + w_y(k) \end{aligned} \tag{14}$$

In the standard form, shown above, direct injection of control input, $u(k)$, and measured disturbance, $w_m(k)$ in the output equation does not exist. In the hybrid fuel cell output equation (12), there is a direct injection of control input. We, therefore, filtered the two inputs through linear first order filters with unity gain and very fast time constants. When these filters are augmented with equations (11) and (12), the number of states increases by two and system matrices change accordingly. As a result, the new system will be in the standard form. In the development below, we assume that the model has been modified in this manner. Therefore for the hybrid fuel cell, the nonlinear plant model (13) is described by:

$$x_p = [x_{nl}, \quad SD, \quad x_u]^T \quad u = [V_{cm}, \quad I_{fc}]^T \quad w_m = I_{des}$$

where x_{nl} is nonlinear fuel cell states given by equation (7), SD is the capacitor state of discharge given by equation (10), and x_u are the two filter states. The unmeasured disturbance, w_u, and the output disturbance, w_y, are assumed to be zero. The linear plant (internal model) (14), is described by:

$$x = [x_{ln}, \quad SD, \quad x_u]^T \quad u = [V_{cm}, \quad I_{fc}]^T \quad w_m = I_{des}$$

where x_{ln} is linear fuel cell states given by equation (8).

The future state of the plant can be estimated using the internal model, assuming that unmeasured disturbances are zero in the future [17]:

$$\begin{aligned} \hat{x}(k+1|k) &= A\hat{x}(k|k-1) + B_u u(k) + B_{wm} w_m(k) + L\hat{d}(k|k) \\ \hat{y}(k|k-1) &= C\hat{x}(k|k-1) + D_{wu} w_u(k) \end{aligned} \tag{15}$$

where $\hat{x}(k+1|k)$ is the estimate of the state at future sampling instant $k+1$ based on information available at instant k, and $\hat{y}(k|k-1)$ is the output estimate at instant k based on information available at instant $k-1$. L is the constant estimator gain and $\hat{d}(k|k)$ is the current value of estimator error:

$$\hat{d}(k|k) = y_p(k) - \hat{y}(k|k-1) \tag{16}$$

One key assumption is that future values of measured disturbance, $w_m(k)$, and calculated estimator error, $\hat{d}(k|k)$, remain constant during the next prediction horizon. In MPC with a control horizon of N and prediction horizon of P, a control sequence

$$u^N = [u(k) \quad u(k+1) \quad \ldots \quad u(k+N-1)]^T$$

is sought at each instant, k, which minimizes the following finite horizon performance index:

$$J = \sum_{j=1}^{P} \left(\|Q(r(k+j) - \hat{y}(k+j|k))\|_2{}^2 + \|S\Delta u(k+j-1)\|_2{}^2 \right) \tag{17}$$

and satisfies the following constraints:

$$\begin{aligned} &u_{min}(j) \le u(k+j) \le u_{max}(j) \quad j = 0, 1, \ldots, N-1 \\ &\Delta u(k+j) \le \Delta u_{max}(j) \quad j = 0, 1, \ldots, N \\ &y_{min}(j) \le \hat{y}(k+j|k) \le y_{max}(j) \quad j = j_1, j_1+1, \ldots, j_2 \end{aligned} \tag{18}$$

In the performance index, S and Q are input and output weighting matrices respectively. Penalizing the change in the input, Δu, automatically adds integral action on the tracking error. At the current sampling instant, k, the plant output, $y_p(k)$, and the disturbance, $w_m(k)$, are measured. The estimation error, $\hat{d}(k|k)$ is calculated using equation (16). Based on the assumption that future values of measured disturbances and estimator errors remain constant during the next prediction horizon, $\hat{y}(k+j|k)$ can be calculated as a function of the control sequence, u^N, only. The performance index (17) and the constraints (18) can be written as functions of u^N and measured outputs, disturbances and the reference command in a quadratic form. Quadratic programming techniques could be used to solve this constrained optimization problem at each sampling time. In absence of constraints, the problem reduces to a simple minimization problem and an explicit control law can be calculated. With constraints, on the other hand, a straightforward explicit control law does not exist. Instead numerical optimization of the performance index is carried out online to find the control input.[3] Simulating a constrained problem normally takes much longer time than the equivalent unconstrained problem. Since the solution depends on iterative numerical procedure, as the constraints become more stringent the computational time increases. So pushing the system to its limits for the best possible performance, might result in very large computational time. Therefore a balance between tightening the constraints and computational resources is necessary.

4.1 Simulation Analysis

In this paper, the linear model described in (11-12) is used to represent the plant and internal models for linear simulations. In nonlinear simulations, the nonlinear model of the fuel cell (7) augmented with (10) is used to represent the plant. First the capabilities of the MPC controller is established for the linearized model of the plant and suitable design parameters, such as performance weights and prediction horizon are determined. The control design is then verified with the actual nonlinear model of the plant. The desired reference command is fixed for all

[3] It can be shown that with linear constraints, the control is a piecewise linear function of the states. However analytical calculation of it becomes increasingly difficult as larger prediction horizons are used [18].

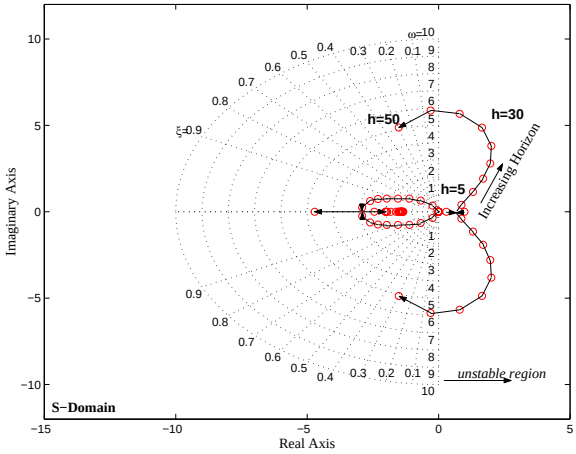

Figure 3: Loci of closed-loop poles in s-domain as prediction horizon increases from 2 to 50 steps. The performance index weights are $Q = diag(100, 0.1)$, $S = diag(0.1, 0.001)$.

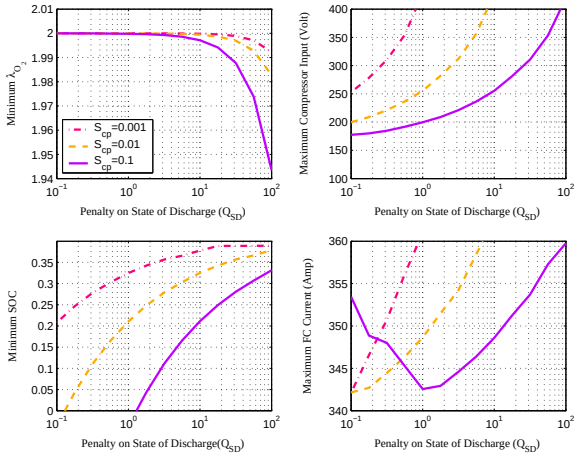

Figure 4: Worst input and output values for different selection of penalty on compressor input, S_{cp}, and penalty on SOC, Q_{SD}, when demand jumps from 191 to 291 Amps. Penalty on oxygen is fixed at $Q_{OER} = 100$ and penalty on current is fixed at $S_I = 0.001$.

times at $r = [0 \quad 0.5]^T$, implying the desired output values of $\lambda_{O_2}^{des} = 2$ and $SOC^{des} = 0.5$. We used a sampling frequency of 100 Hz. The length of prediction horizon is influential in both the computational time and performance of the system. Figure 3 shows the influence of choice of prediction horizon on performance in linear unconstrained simulations. The loci of the dominant poles are shown in the s-domain as prediction horizon is increased from two to fifty sampling times. It is clearly shown that, a short prediction horizon results in a pair of unstable closed loop poles. This behavior is due to dynamics of state of charge which is a simple integrator. If the state of charge is not heavily penalized and if the prediction horizon is short, the controller will use the capacitor aggressively to regulate the air flow in this short horizon. The "short-sighted" and aggressive use of the capacitor can result in an unstable closed-loop system. Based on this analysis we chose 50 sampling instants for the prediction horizon to avoid such undesirable performance for different levels of capacitor utilization.[4]

Consider $Q = diag(Q_{OER}, Q_{SD})$ and $S = diag(S_{cp}, S_I)$ in the performance index (17), where Q_{OER}, Q_{SD}, S_{cp} and S_I are penalties on oxygen excess ratio, state of discharge, compressor input and current drawn from the fuel cell, respectively. The weight on the state of discharge determines the extent to which the capacitor is used. Small weights allow full use of the capacitor and large weights restrict full discharge of the capacitor. Figure 4 shows the influence of the weights on maximum deviation from nominal values of inputs and outputs as the current demand increases from 191 to 291 Amps. In each plot, the x-axis shows the penalty on the state of discharge and each curve corresponds to a different penalty on compressor voltage. Penalty on OER is fixed at 100 and penalty on current is fixed at 0.001. Based on this plot, we chose the penalty on state of charge to be 1 and the penalty on compressor at 0.1. This values result in good oxygen regulation with minimum compressor use (less than 200 volts) and maximum utilization of the ultracapacitor (minimum SOC equal to zero) for 100 Amps increase in current. Therefore for the rest of simulations, the penalty matrices $Q = diag(100, 1)$ and $S = diag(0.1, 0.001)$ are fixed. As an extra measure, hard constraints could be enforced on the capacitors state of charge, to ensure that it is not overcharged or over-drained. In this paper we compare both the unconstrained and constrained case in simulations.

Figure 5 shows the linear and nonlinear simulation results during step changes in current demand. No constraint is imposed in this set of simulations. During step changes in the demand, the capacitor is used to meet the sudden increase in demand. In this stage, the current drawn from the fuel cell, I_{fc}, is less than the demand current, I_{des}, but rises smoothly to catch up with the demand. As a result oxygen deficit reduces to negligible levels as shown in linear and nonlinear simulations. When the fuel cell current tops the demand, the capacitor starts to recharge. It is important that the state of charge remains within feasible bounds under the anticipated current demands. Increasing the penalty on state of charge reduces this possibility, but does this only by limiting the use of the capacitor even at low current levels. To utilize a capacitor to its maximum degree without overriding its limits, explicit constraints should be included on state of charge. Indeed one main advantage of model predictive control design is its potential to optimize in presence of such output constraints. As an example, we set tight bounds of 0.35 and 0.65 on state of charge in a new MPC design.

With constraints, an straightforward closed-form solution does not exist and the control input is calculated online by constraint-optimization of the performance index. The linear predictive model is used for online prediction and the nonlinear plant outputs are used to update the outputs of this linear predictor. Simulation results are shown in Figure 6. The state of charge has remained between the pre-specified bounds in linear and nonlinear simulations. Maintaining state of charge within limits, prevents undesirable voltage variations across the capacitor. Moreover, a less conservative design is possible by constrained optimization which allows a reduction in the size of the capacitor without loss of performance.

5 Conclusions

In this paper, inclusion of a fast-responding auxiliary power source was proposed to prevent oxygen starvation in a fuel cell during rapid current transitions. In the hybrid architecture, the current drawn from the fuel cell was regulated and the deficit was compensated by an ultra-capacitor. A model predictive control design was used in this

[4] In a model predictive control design, stability is guaranteed if the original open-loop plant is stable. Otherwise extra requirements need to be fulfilled to achieve closed-loop stability [19]. Using an infinite prediction horizon is one way of ensuring stability. In practice increasing the length of the prediction horizon is a common way in industry to enhance the stability properties of the system [20].

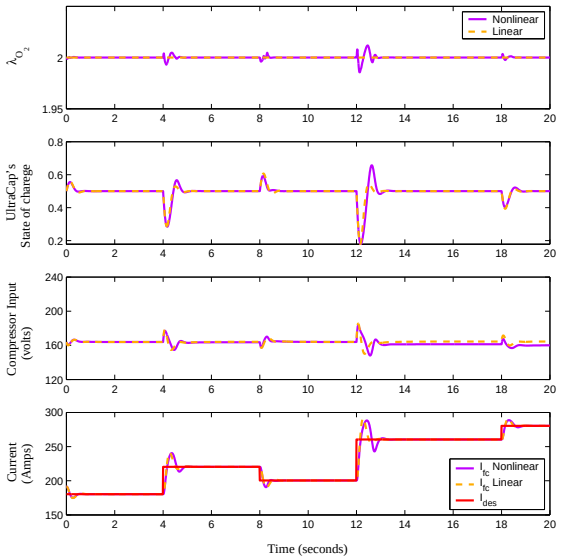

Figure 5: Performance of the hybrid system. No constraint is enforced. The performance index weights are $Q = diag(100,1)$, $S = diag(0.1,0.001)$.

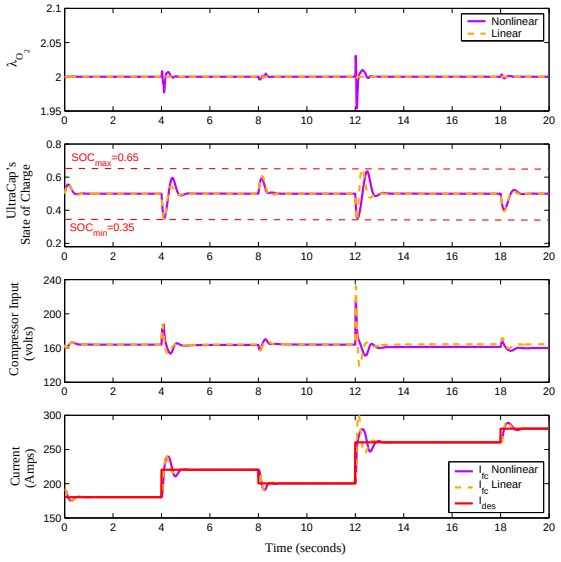

Figure 6: Performance of the hybrid system with output constraint on state of charge. The performance index weights are $Q = diag(100,1)$, $S = diag(0.1,0.001)$.

architecture for optimal distribution of current demand between the resources. Choice of model predictive control over conventional control methodologies was motivated by two key requirements: 1) Smoother decisions in resource allocation despite unknown load cycles 2) Handling constraints of auxiliary power source. The controller performed well in splitting the demand between the fuel cell and the capacitor. As a result, the reactant deficit during a 100 Amp increase in current demand reduced from 50% in stand-alone architecture, as shown in Figure 2, to less than 1% in the hybrid configuration, as shown in Figure 4. MPC allowed enforcing operational constraints on capacitor's state of charge. The design was verified on a detailed nonlinear model of the fuel cell system. It was shown that the hybrid architecture together with constraint-handling capabilities of model predictive control, provides a versatile design for achieving different requirements on the performance variables. This goal is met without assuming a-priori knowledge of the load cycle.

6 Acknowledgements

The authors thank Dr. Ilya Kolmanovsky at Ford Motor Company for his helpful advice and feedbacks.

References

[1] J. Pukrushpan, A. Stefanopoulou, and H. Peng, "Modeling and control for PEM fuel cell stack system," *Proceedings of American Control Conference*, 2002.

[2] J. Sun and I. Kolmanovsky, "A robust load governor for fuel cell oxygen starvation protection," *Proceedings of the American Control Conference*, June 2004.

[3] E. Gilbert and I. Kolmanovsky, "Nonlinear tracking control in the presence of state and control constraints: a generalized reference governor," *Automatica*, vol. 38, pp. 2063–2073, 2002.

[4] N. Jalil, N.A. Kheir, and M. Salman, "A rule-based energy management strategy for a series hybrid vehicle," *Proceedings of American Control Conference*, pp. 689–693, 1997.

[5] Z. Fillipi, L. Louca, A. Stefanopoulou, J. Pukrushpan, B. Kittirungsi, and H. Peng, "Fuel cell APU for silent watch and mild electrification of a medium tactical truck," *SAE Paper No 2004-01-1477*, 2004.

[6] C.C. Lin, J.M. Kang, J.M Grizzle, and H. Peng, "Energy management strategy for a parallel hybrid electric truck," *Proceedings of the American Control Conference*, pp. 2878–2883, 2001.

[7] A. Brahma, Y. Guezennec, and G. Rizzoni, "Optimal energy management in series hybrid electric vehicles," *Proceedings of the American Control Conference*, pp. 60–64, 2000.

[8] P. Rodatz, O. Garcia, L. Guzzella, F. Buchi, M. Bartschi, A. Tsukada, P. Dietrich, R. Kotz, G. Scherer, and A. Wokaun, "Performance and operational characteristics of a hybrid vehicle powered by fuel cells and supercapacitors," *SAE Paper 2003-01- 0418*, 2003.

[9] T. Matsumoto, N. Watanabe, H. Sugiura, and T. Ishikawa, "Development of fuel-cell hybrid vehicle," *SAE Paper No. 2002-01-0096*, 2002.

[10] L.P. Jarvis, P.J. Cygan, and M.P. Roberts, "Hybrid power source for manportable applications," *IEEE AESS Systems Magazine*, pp. 13–16, 2003.

[11] G. Paganelli, T.M. Guerra, S. Delprat, Y. Guezennec, and G. Rizzoni, "Optimal control theory applied to hybrid fuel cell powered vehicle," *Proceedings of IFAC 15th Triennial World Congress*, 2002.

[12] J. Pukrushpan, H. Peng, and A. Stefanopoulou, "Simulation and analysis of transient fuel cell system performance based on a dynamic reactant flow model," *Proceedings of 2002 ASME International Mechanical Engineering Conference and Exposition*, vol. IMECE2002-DSC-B32051, also in "Modeling and Analysis of Fuel Cell Reactant Flow for Automotive Applications, to appear in ASME Journal of Dynamic Systems, Measurement and Control, vol. 126, June 2004".

[13] S. Piller, M. Perrin, and A. Jossen, "Methods for state-of-charge determination and their applications," *Journal of Power Sources*, vol. 96, pp. 113–120, 2001.

[14] A. Burke, "Ultracapacitors: why, how, and where is the technology," *Journal of Power Sources*, vol. 91, pp. 37–50, 2000.

[15] J.H. Lee and N.L. Ricker, "Extended kalman filter based nonlinear model predictive control," *Industrial and Engineering Chemistry Research*, vol. 33, pp. 1530–1541, 1994.

[16] N.L. Ricker and J.H. Lee, "Nonlinear model predictive control of the tennessee eastman challenge process," *Computers and Chemical Engineering*, vol. 19, pp. 961–981, 1995.

[17] N.L. Ricker, "Model predictive control with state estimation," *Industrial and Engineering Chemistry Research*, vol. 29, pp. 374–382, 1990.

[18] P. Tondel, T. Johansen, and A. Bemporad, "An algorithm for multi-parametric quadratic programming and explicit MPC solutions," *Automatica*, vol. 39, no. 3, pp. 489–497, March 2003.

[19] K.R. Muske and J.B. Rawlings, "Model predictive control with linear models," *Process Systems Engineering*, vol. 39, no. 2.

[20] D.W. Clarke, *Advances in Model-Based Predictive Control*, Oxford University Press, 1994.